POLAROGRAPHY OF THE OXYTOCIN AND VASOPRESSIN SYNTHETIC ANALOGS

Pavel MADER[a], Věra VESELÁ[b], Michael HEYROVSKÝ[c], Michal LEBL[d] and Milena BRAUNSTEINOVÁ[e]

[a] *Faculty of Agronomy, University of Agriculture, 165 21 Prague 6-Suchdol*
[b] *Institute of Experimental Physics, Slovak Academy of Sciences, 043 53 Košice*
[c] *The J. Heyrovský Institute of Physical Chemistry and Electrochemistry, Czechoslovak Academy of Sciences, 118 40 Prague 1*
[d] *Institute of Organic Chemistry and Biochemistry, Czechoslovak Academy of Sciences, 166 10 Prague 6 and*
[e] *Léčiva, n.p., závod 04, 180 47 Prague 9*

Received June 29th, 1987
Accepted February 8th, 1988

Small changes in the molecules of the oxytocin and vasopressin synthetic analogs bring about considerable changes in their polarographic behavior within the entire potential interval available (+0·5 to −2·0 V vs SCE). In the study of the polarographic activity of ten peptides we used classical, differential pulse and alternating current polarography and cyclic voltammetry. Liquid chromatographic separation studies of the peptides on the reverse phase complemented the electrochemical investigation. Hydrophobicity showed to be the parameter which decisively influences the polarographic behavior of the studied peptides. Strong interaction of the SS and S-carba analogs with the electrode material (mercury) has been observed and surface activity of the SH-forms of the peptides at negative potentials has been confirmed. The importance of various functional groups in the peptide molecule for the catalytic activity in hydrogen evolution at negative potentials is discussed.

The natural neurohypophyseal hormones oxytocin and vasopressin and their synthetic analogs have been subjects of intensive studies for decades. Results of these studies were recently summarized and extensively discussed in a monograph[1]. Besides the biological activity and synthesis, considerable effort is also being devoted to the investigation of many other properties of these peptides, in particular, to their physico-chemical characteristics. The main reason for it is the effort to establish a ground on basis of which it would be possible to predict biological activity of various synthetic analogs, the ultimate goal being the design of new analogs with the ideal properties, for example with so-called "absolute specificities". Hence, correlations of their activities with a number of other properties are closely followed, with the hope to disclose those which mainly or ultimately reflect their biological effects. Among many physico-chemical methods, the spectroscopic ones clearly dominate but various other methods including, e.g., liquid chromatography, diffusion through the membranes or binding experiments are also frequently used. In this connection it is surprising that the electrochemical methods have been used only marginally regardless of the fact that the intramolecular SS-bond, present in all natural neuro-hypophyseal hormones and in a large majority of their synthetic analogs, yields a characteristic polarographic

reduction wave at mercury and other electrodes. Further, we can also expect a catalytic effect of the above peptides in the polarographic reduction of hydrogen, in analogy with many smaller and larger peptides as well as proteins. Finally, small modifications in the peptide molecule, known to bring about fundamental changes in their biological activity, may also affect the course of the electrochemical SS-bond reduction and/or other electrochemical characteristics of these peptides. So far, polarography has been used in several instances only. Thus, in 1969, Krupička and Zaoral[2] described the DC-polarographic behavior of the natural nonapeptides [8-lysine]-vasopressin and [8-arginine]vasopressin and also of their synthetic analogs [1-β-mercaptopropionic acid, 8-D-α,γ-diaminobutyric acid]vasopressin and [1-β-mercaptopropionic acid, 8-D--arginine]vasopressin. In 1975, Rishpon and Miller[3,4] studied adsorption and electrode reactions of oligopeptides oxytocin, deaminooxytocin and [8-lysine]vasopressin at the dropping mercury electrode and, in 1984, Forsman[5,6] described cathodic stripping voltammetry of oxytocin, [8-lysine]vasopressin, [2-phenylalanine, 8-lysine]vasopressin and several other compounds from the point of view of quantitative determination of minute amounts of these compounds.

In this paper, we present results of our own investigation of the polarographic activity of ten peptides: oxytocin, seven of its synthetic analogs (including three carba analogs), and two analogs of vasopressin. In distinction to the above quoted papers[2–6] we did not restrict our study to the area of the S—S bond reduction only but covered the entire potential range available. Thus, five distinct potential regions were investigated and discussed: the zero-charge region, the region of the positively charged electrode surface (i.e., the region of the reference electrode potential), and the region of the negatively charged electrode surface which we divided into three parts – the region of the S—S bond reduction, the region of the catalyzed hydrogen discharge, and the region in-between. The behavior of the peptides at the uncharged electrode was followed with particular interest as the hydrophobicity of the peptide molecule and the chemisorption interaction between the peptide and the electrode are not disturbed by the electrostatic interactions and/or by the splitting of the S—S bond. For better elucidation of the possible role of hydrophobicity we performed also liquid chromatographic separation of the peptides on reverse

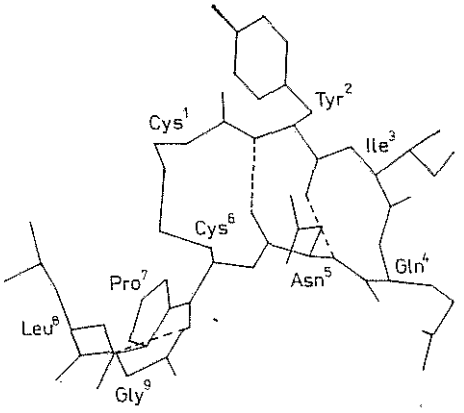

FIG. 1

Conformation of the peptide *V* determined in crystal. According to Wood et al.[7]

phase. Since other physicochemical methods have provided evidence for very similar conformational and dynamic properties of the studied peptides (see ref.[1]) it was assumed that different retention on reverse phase can be explained by different hydrophobicities of various amino acid side chains.

As concerns conformation, the contemporary ideas, supported by the recent determination of the crystal structure of deaminooxytocin, view a structure which contains a β-turn consisting of the amino acids Tyr-Ile-Gln-Asn, and is stabilized by the intramolecular hydrogen bond between the carbonyl of tyrosine and the backbone NH of asparagine (see Fig. 1). In aqueous solutions, all these peptides are conformationally very flexible. The only peptide amide proton that appears to be significantly solvent shielded in aqueous solutions is the Cys^6 proton. The Asn^5 peptide amide proton also may be shielded to a small extent. Most of the oxytocin analogs as well as arginine- and lysine-vasopressin have very similar conformations about the disulfide bond. The above conclusions of the experimental investigations have been confirmed also by calculations of the energy content of various conformations in water.

At the charged electrode surface, electrostatic interactions between the electrode and electrically charged groups in the peptide molecule contribute to the overall electrochemical activity of the peptides. The amidic group of the peptide chain is electrically neutral. Oxytocin with the NH_2-group or with the modified terminal NH_2-group is always electrically uncharged. The value of pK of the α-amino group decreases considerably in the vicinity of the disulfide group (e.g., pK of diglycylcystin is 7·94, that of cystinylglycine as low as 6·36). For oxytocin literature states the value of 6·3 (ref.[1]). The value of pK for arginine is 12·48 and for lysine 10·53 (ref.[8]). Having had such broad spectrum of basically similar peptides it was our interest also to see the importance of various functional groups in the peptide molecule for the resulting catalytic activity in the hydrogen evolution reaction. This question was raised, a.o., by Millar[9] and the role of sulfur in this type of catalytic activity has not been completely elucidated until today.

EXPERIMENTAL

All the ten peptides studied were of synthetic origin. Their chemical names, summary formulas, and literature dealing with their synthesis and basic properties, are surveyed in Table I. Storage solutions of the peptides in concentrations $1 . 10^{-2}$, $1 . 10^{-3}$ and $1 . 10^{-4}$ mol l^{-1} have been prepared by dissolution of the peptides in $1 . 10^{-2}$ mol l^{-1} HCl. The solutions were stored in the refrigerator.

According to the information of the producer the supplied samples of the peptides contained always variable amounts of acetic acid (max. 4 molecules) and water (max. 6 molecules in one molecule of the peptide). This represents a contribution of min. 78 (1 CH_3COOH + 1 H_2O) and max. 348 (4 CH_3COOH + 6 H_2O) to the molecular mass of the peptide. The smallest of them (peptide *VII*) had m.w. 988, the largest one (peptide *IX*) m.w. 1 227. The values of peptide concentrations stated in this paper are derived from the amounts of the weighted aliquots of the

supplied samples with the presence of either CH_3COOH or H_2O in their molecule neglected. With respect to the above given values, the actual concentrations of the peptides in solutions prepared by us in this study are always lower than we state, the difference being at least 6% and at most 26%. Since we had at our disposal only minute amounts of the peptide samples (units and tens of mg), we could not determine more precisely their concentrations in the studied solutions. With respect to the above variability (6 to 26%) we also did not perform correction for dilution, which represented 0·5 to 5%.

Crystalline sodium tetraborate, boric acid and hydrochloric acid were all products of Lachema Brno, Czechoslovakia. All reagents used were of analytical reagent purity. Water was doubly distilled.

For the DC- and DP-polarography we used the polarographic analyzers PA-2 or PA-3 and the XY-recorder model XY-4 103, all products of Laboratorní přístroje Prague, Czechoslovakia. The scan rate was 2 or 5 mV s^{-1} and the forced drop time 2 s; the flow of mercury did not exceed 2 mg s^{-1}. The polarization pulse in DP-measurements amounted to −50 mV.

Phase-sensitive AC-polarograms were recorded with the help of the GWP-673 polarograph and the ENDIM 62 002 recorder, both products of the Zentrum für wissenschaftliche Gerätebau Berlin, G.D.R. The non-tast regime of the AC-curves has been used with damping 5, time of the forced drop 4 s, flow of mercury 1·1 mg s^{-1}. The scan rate equalled 8·3 mV s^{-1}.

Cyclic voltammetry was performed with the hanging mercury drop electrode SMDE-1 combined with the analyzer PA-3 and recorder XY-4 103, all products of Laboratorní přístroje Prague, Czechoslovakia. The growth time of one drop used was always 160 ms. With the excep-

TABLE I
List of the studied peptides

Peptide denot.	Chemical name	Summary formula	Ref.[a]
I	oxytocin	$C_{43}H_{66}N_{12}O_{12}S_2$	—
II	[2-O-methyltyrosine]oxytocin	$C_{44}H_{68}N_{12}O_{12}S_2$	10
III	N-CH_3CO-[2-O-methyltyrosine]oxytocin	$C_{46}H_{70}N_{12}O_{13}S_2$	11
IV	N-$(CH_3)_3CCO$-[2-O-methyltyrosine]oxytocin	$C_{49}H_{76}N_{12}O_{13}S_2$	12
V	deamino-oxytocin	$C_{43}H_{65}N_{11}O_{12}S_2$	13
VIa	[2-(L-*p*-ethylphenylalanine)]deamino-6-carba-oxytocin	$C_{46}H_{71}N_{11}O_{11}S$	14
VIb	[2-(D-*p*-ethylphenylalanine)]deamino-6-carba-oxytocin	$C_{46}H_{71}N_{11}O_{11}S$	15
VII	[2-O-methyltyrosine]deamino-1-carba-oxytocin	$C_{46}H_{69}N_{11}O_{12}S$	16
VIII	[8-D-arginine]deamino-vasopressin	$C_{46}H_{64}N_{14}O_{12}S_2$	17
IX	glycyl-glycyl-glycyl-[8-lysine]vasopressin	$C_{52}H_{74}N_{16}O_{15}S_2$	18

[a] Papers dealing with synthesis and properties of the respective peptides.

tion of cases when we studied the effect of accumulation the 1st cycle was begun always immediately after the formation of a new drop.

Instantaneous current vs time curves were recorded with mutually interconnected analyzers PA-2 and PA-3. For logarithmic analysis we used only currents recorded one second and further after the beginning of the drop[19].

Unless otherwise stated, saturated calomel electrode served as the reference electrode. During AC-polarography, the auxiliary electrode was formed by the bottom mercury, in all other cases platinum sheet was used.

Liquid chromatography on the reversed phase was performed with the instrument SP-8 700 furnished with the spectrophotometric detector SP-8 400 and the integrator SP-4 100 (Spectra Physics, Santa Clara, U.S.A.). We used the 25 × 0·4 cm column with Separon SIC-18 7 μm (Laboratorní přístroje Prague, Czechoslovakia). For elution the methanol gradient of 2 vol. % min^{-1} was used, which began either with 25 vol. % methanol (when the buffer of pH 2·2, i.e., 0·05 vol. % trifluoroacetic acid, was used), or with 50 vol. % methanol (buffer 0·1 mol l^{-1} CH_3COONH_4, pH 7·5). Peptides were analyzed both separately and together.

RESULTS

Region of the Non-Faradaic Phenomena

In order to obtain information about the behavior of peptides on the mercury/solution interface also at potentials at which they do not get reduced, we recorded polarographic curves from the potential of the anodic mercury dissolution. Polarograms of the peptides *I*, *II*, *III*, *V*, *VII*, *VIII*, and *IX* in concentrations of $2 . 10^{-5}$ and $2 . 10^{-4}$ mol . $. l^{-1}$ were compared with the curve for the blank alone (0·05M-borax, 0·5M-H_3BO_3, pH 7·4). Results obtained with mean currents have been evaluated in detail for peptide *III* with the help of the instantaneous current vs time curves. All tested peptides exhibit small cathodic non-Faradaic current which is a consequence of their specific interaction with the electrode surface in the potential interval from the mercury dissolution to the SS-reduction wave. Beginning of the rise of the anodic current, corresponding to the dissolution of mercury, is shifted to variable extent towards the more negative potentials in the presence of the peptides, but this shift never exceeds 50 mV. The anodic wave is not formed. Peptides which yield higher cathodic current of this interaction (the highest current was observed in the presence of peptide *VII*) influence less the anodic dissolution of mercury.

Region of the Faradaic Phenomena

Reduction of the SS-*Group*

DC-*polarography*: With the exception of the carba analogs (peptides *VIa*, *VIb*, and *VII*) all studied peptides gave well developed cathodic wave at potentials c. −0·6 to −0·8 V vs SCE (depending on pH and peptide concentration); this cathodic wave obviously belongs to the reduction of the disulfide group. Limiting current of this

wave is purely diffusion controlled in nature, as follows from the measurements of its dependence on height of the mercury reservoir and on temperature; the above conclusion is supported also by the course of the instantaneous current vs time curves, which are monotonous parabolas with the exponent, x, in the expression $i = kt^x$ close to 0·17. Also the dependence on the peptide concentration was linear in the whole concentration region tested ($3 . 10^{-5}$ to $5 . 10^{-4}$ mol l^{-1}, with peptide *VIII* $1 . 10^{-5}$ to $1 . 10^{-3}$ mol l^{-1}).

The values of $E_{1/2}$ at pH 7·4 for several concentrations of the peptides are given in Table II. With increasing peptide concentration the half-wave potential is initially (between $3 . 10^{-5}$ and $1 . 10^{-4}$ mol l^{-1} peptide) shifted towards the less negative values, but at higher peptide concentrations the direction of this shift becomes reversed; upon change of the peptide concentration from $1 . 10^{-4}$ to $5 . 10^{-4}$ mol l^{-1} and in the region of pH 7·4 to 9·2 the shift of $E_{1/2}$ amounts to 20 to 70 mV depending on the peptide.

Effect of pH on $E_{1/2}$ was studied in detail with peptide *VIII* only; between pH 7·4 and 9·2, $E_{1/2}$ was shifted negatively with increasing pH, the increment for unit pH being c. 60 mV at lower (1 and $2 . 10^{-4}$ mol l^{-1}) and c. 40 mV at higher ($6 . 10^{-4}$ mol. . l^{-1}) concentrations of peptide *VIII*.

Logarithmic analysis of the S—S reduction wave yielded mostly single line whose coefficient of linear correlation, r, was higher than 0·99. Peptide *III* was an exception since it gave two distinct linear segments, whose slopes differed considerably from each other. Also here, the values of the coefficient r for both linear segments considerably exceeded 0·99; the linear regression analysis of the whole correlation field yielded the lines with $r = 0·978$ or less (Fig. 2). At pH 7·4 and peptide concentration

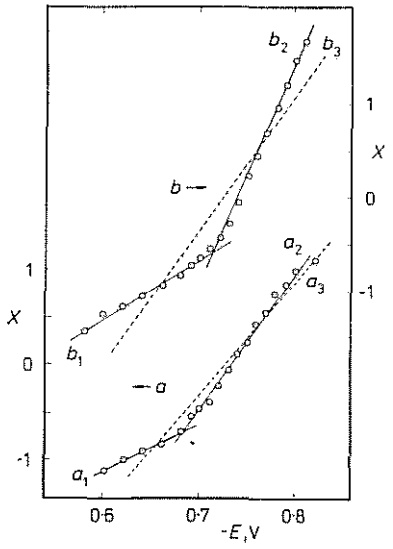

FIG. 2

Logarithmic analysis ($X \equiv \log (I/(I_d - I))$) of the peptide *III* reduction wave at pH 9·2. Values for mean currents. Peptide concentration (in 10^{-4} mol l^{-1}): *a* 1; *b* 2. Inverse value of the slope, $1/s$ (in mV), coefficient of correlation, r: a_1 201·9, 0·9946; a_2 70·6, 0·9956; a_3 84·9, 0·9783; b_1 158·6, 0·9929; b_2 42·9, 0·9965; b_3 70·4, 0·9401

$1 . 10^{-4}$ mol l^{-1}, the value of the slope of the above line increased in the sequence peptide *V* (84·7) – *VIII* (87·8) – *IV* (103·4) – *IX* (117·4) – *III* (125·5) – *II* (130·1) – *I* (151·2 mV). Changes in the slope value with peptide concentration were monotonous (decrease upon increasing concentration of the peptide) only in the case of peptides *III*, *IV*, and *V* (i.e., peptides of the oxytocin type with modified terminal NH_2-group). Decrease of pH from 9·2 to 7·4 had practically no effect on the value of the slope of peptide *VIII*, increased slightly the slope of peptide *IX* (20 to 30 mV increase depending on the peptide concentration) and increased somewhat more the value of the slope of peptides *II* (increase 15 to 85mV) and *III* (increase 50 to 60 mV).

We consider important our finding that the DC-polarograms at potentials of the foot of the SS-reduction wave of peptides *I*, *II*, *III*, and *IX* were often accompanied by characteristic irregularities (several examples see in Fig. 3 above); with peptide *III* in higher concentrations (3 and $5 . 10^{-4}$ mol l^{-1}) even the well developed prewave separated out from the main reduction wave. The irregularities manifested themselves particularly on the course of the instantaneous current vs time curves. Under the experimental conditions used in this study, no indication of any irregularities of the above type has been observed with peptides *IV*, *V*, and *VIII*.

DP-*polarography*: DP-polarograms were recorded with peptides *I*, *II*, *III*, *VIII*, and *IX*. All of them gave distinct DP-peak at potentials close to the value of $E_{1/2}$ for the DC-reduction wave of the SS-group under the same experimental conditions. Again, peptides *I*, *II*, and *III* often exhibited irregular behavior at potentials of the foot of the SS-reduction wave. Under the DP-regime, these irregularities manifested themselves, e.g., by the presence of one or two shoulders on the foot(s) of the DP-peak; by marked asymmetry of the DP-peak; or by the presence of a well-developed independent DP-peak preceding the main DP-peak. Examples of all three above specified types of the irregular behavior are shown in Fig. 3 (bottom). While the height of the (main) DP-peak always increases linearly with increasing concentration of the peptide, the additional preceding small DP-peak increases with the exponent less than one. Under the used experimental conditions, peptides *VIII* and *IX* never gave any indication of the above or another type of the irregular behavior.

Cyclic voltammetry: Cyclic voltammograms were recorded at pH 7·4 and in the concentration interval between $3 . 10^{-5}$ and $5 . 10^{-4}$ mol l^{-1} (peptides *I*, *II*, *III*, *VIII*, and *XI*), or $1·5 . 10^{-5}$ and $1 . 10^{-4}$ mol l^{-1} (peptides *IV* and *V*). The investigated potential region was at most 0 to −1·6 V, scan rate 20 to 200 mV s^{-1}.

With peptide *III* in concentration $3 . 10^{-5}$ mol l^{-1} and at scan rate 100 mV s^{-1}, the first cycle yielded single cathodic (C) and single anodic (A) peaks at −0·75 and −0·76 V, resp. With the other peptides, one or two additional side peaks or shoulders were always present on both the cathodic and anodic branches of the cyclic voltammograms; we denote these side peaks or shoulders with the indexes p

TABLE II

Comparison of the values for potential of the main cathodic peak, E_C, in cyclic voltammetry with those for half-wave potential, $E_{1/2}$, in DC-polarography (mV vs SCE), pH 7·4.

Peptide conc. $.10^5$ mol l^{-1}	Scan rate mV s^{-1}	*I*	*II*	*III*	*IV*	*V*	*VIII*	*IX*
		$-E_C-E_{1/2}$	$-E_C-E_{1/2}$	$-E_C-E_{1/2}$	$-E_C-E_{1/2}$	$-E_C-E_{1/2}$	$-E_C-E_{1/2}$	$-E_C-E_{1/2}$
	20	—	—	—	715	720	—	—
1·5	50	—	—	—	710	730	—	—
		—	—	—	—	—	—	—
	100	—	—	—	735	740	—	—
	200	—	—	—	740	730	—	—
	20	685	715	755	710	720	770	780
3	50	680	710	745	720	725	750	760
		668	655	679	—	—	682	730
	100	670	705	740	720	730	750	755
	200	675	715	720	725	720	760	755

	20	680		745		810		720		730		750		790		
6	50	675		690		735		735		740		745		760		
			633		640		672		623		662		649		680	
	100	670		690		780		730		730		735		775		
	200	685		705		760		740		725		745		770		
	20	705		755		780		730		740		780		830		
10	50	690		722		780		730		755		780		800		
			620		622		659		635		674		648		664	
	100	692		717		775		745		750		785		805		
	200	695		730		765		745		785		798		808		
	20	705		755		745		—		—		775		830		
30	50	710		735		755		—		—		795		830		
			641		644		686		—		—		670		671	
	100	710		750		780		—		—		790		835		
	200	715		755		790		—		—		820		840		
	20	770		790		840		—		—		815		850		
50	50	780		805		850		—		—		820		830		
			664		664		713		—		—		693		686	
	100	770		800		865		—		—		820		840		
	200	770		810		875		—		—		840		845		

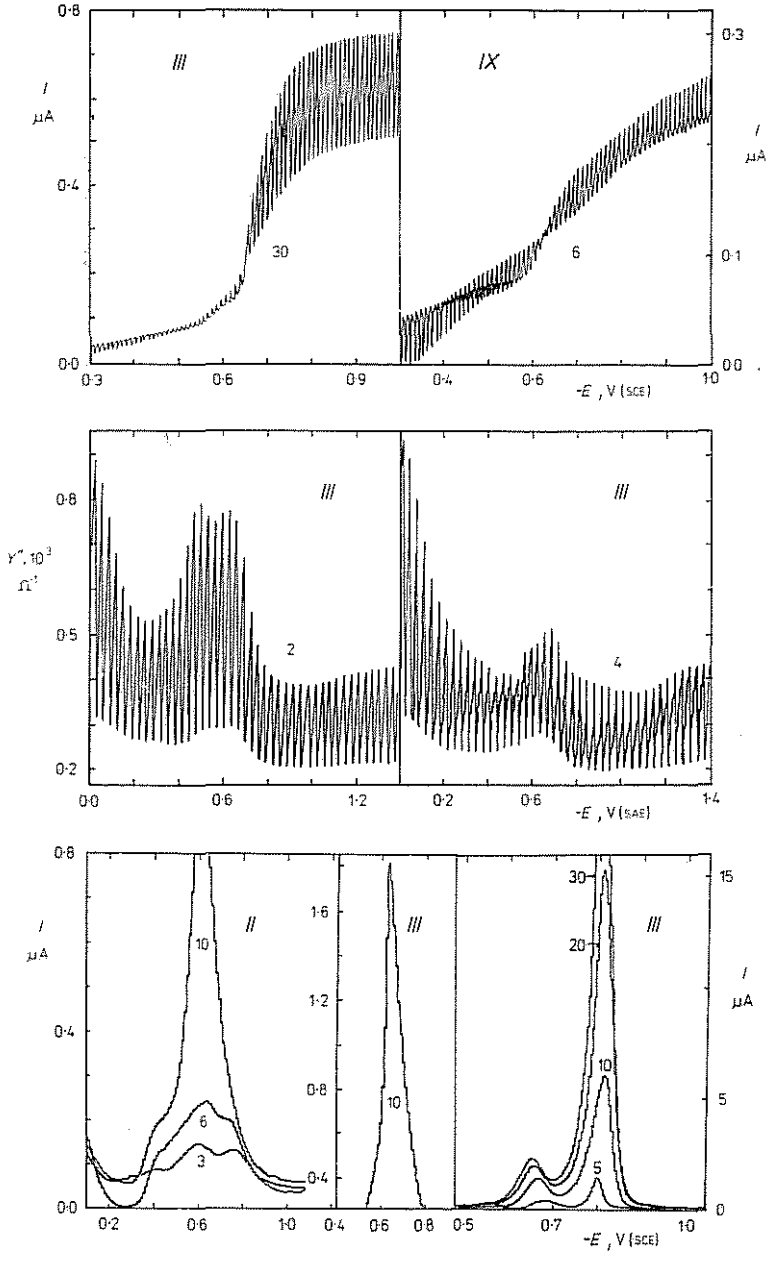

FIG. 3

Examples of irregularities on polarographic records. 0·12 mol l^{-1} borate buffer. Above: DC, pH 7·4, peptides *III* and *IX*; middle AC, pH 7·4, peptide *III*; bottom left DP, pH 7·4, peptide *II*; bottom center DP, pH 7·4, peptide *III*; bottom right DP, pH 9·2, peptide *III*. Numbers at curves denote peptide concentration (in 10^{-5} mol l^{-1})

(more positive) or n (more negative) depending on their position as compared to the main cathodic or anodic peak C or A, resp. Both the main peaks A and C of the peptide *III* and the side anodic peak A_p of this peptide have exceptionally sharp shape, as shown in Fig. 4 left.

With increasing peptide concentration the height of the main cathodic peak C always linearly increases. The main anodic peak A also rises, but only at lower peptide concentrations (up to c. $1 . 10^{-4}$ mol l^{-1}) while at higher peptide concentrations it ceases to grow and remains practically constant. Also the side anodic peaks A_n and A_p rise only at lower peptide concentrations, the only exception being the A_p peak of the peptide *II*.

The value of potential of the main anodic peak A is practically independent of the peptide concentration. The difference between the potentials of the main cathodic (C) and main anodic (A) peaks, ΔE, increases with increasing concentration of the peptide. Thus, for peptide *III* at scan rate 100 mV s^{-1} the value ΔE grew from −10 mV through 0, 20, and 30 mV to 120 mV at concentrations of this peptide of 3, 6, 10, 30, and $50 . 10^{-5}$ mol l^{-1}. Similar values of the ΔE were found also for peptides *III*, *IV*, and *V*. Influence of the scan rate was small and often not monotonous.

Upon increasing the scan rate, the height of the main peaks A and C of all peptides increases monotonously with the exponent less than one. The side peaks C_p, C_n, A_p, and A_n become more distinct at higher scan rates.

The influence of the initial and reversal potentials on the first cycle was studied at the peptide concentration $1 . 10^{-4}$ mol l^{-1} and the scan rate 100 mV s^{-1}. Shift of the initial potential from the usual 0 V to more negative values (up to the foot of the main cathodic wave C) had no effect; analogously, the positive shift of the reversal potential from the usual −1·5 V up to −0·9 V had no influence on the shape and size of the peaks on cyclic voltammograms of the studied peptides.

Effect of peptide cumulation on the surface of the hanging drop was studied both in the stirred and unstirred solutions. Peptide concentration was $8 . 10^{-5}$ mol l^{-1} for peptide *IV* and $1 . 10^{-4}$ mol l^{-1} for the other peptides, scan rate mostly 100 mV s^{-1}. Cumulation time was 240 s or less, cumulation potential varied between 0 and −0·7 V. Under these conditions, we never observed any changes in cyclic voltammetric behavior with peptides *III*, *V*, and *VIII*. After cumulation at −0·3 and −0·5 V, the main peak C of the peptide *IX* was shifted to more negative potentials (Fig. 5). With the peptides *I*, *II*, and *IV*, cumulation sometimes led to the increase of height of the peak C. In stirred solutions, a new shoulder on the peak C of the peptides *I* and *IV* was created (Fig. 5).

The anodic branches of cyclic voltammograms of the 1st and 2nd (immediately repeated) cycles were always identical. On the other hand, the cathodic branch of the 2nd cycle always exhibited the new peak or shoulder which was absent in the 1st cycle (see dashed line in Fig. 4).

AC-*polarography*: Effect of peptide concentration and effect of frequency of the superimposed voltage have been followed using this technique.

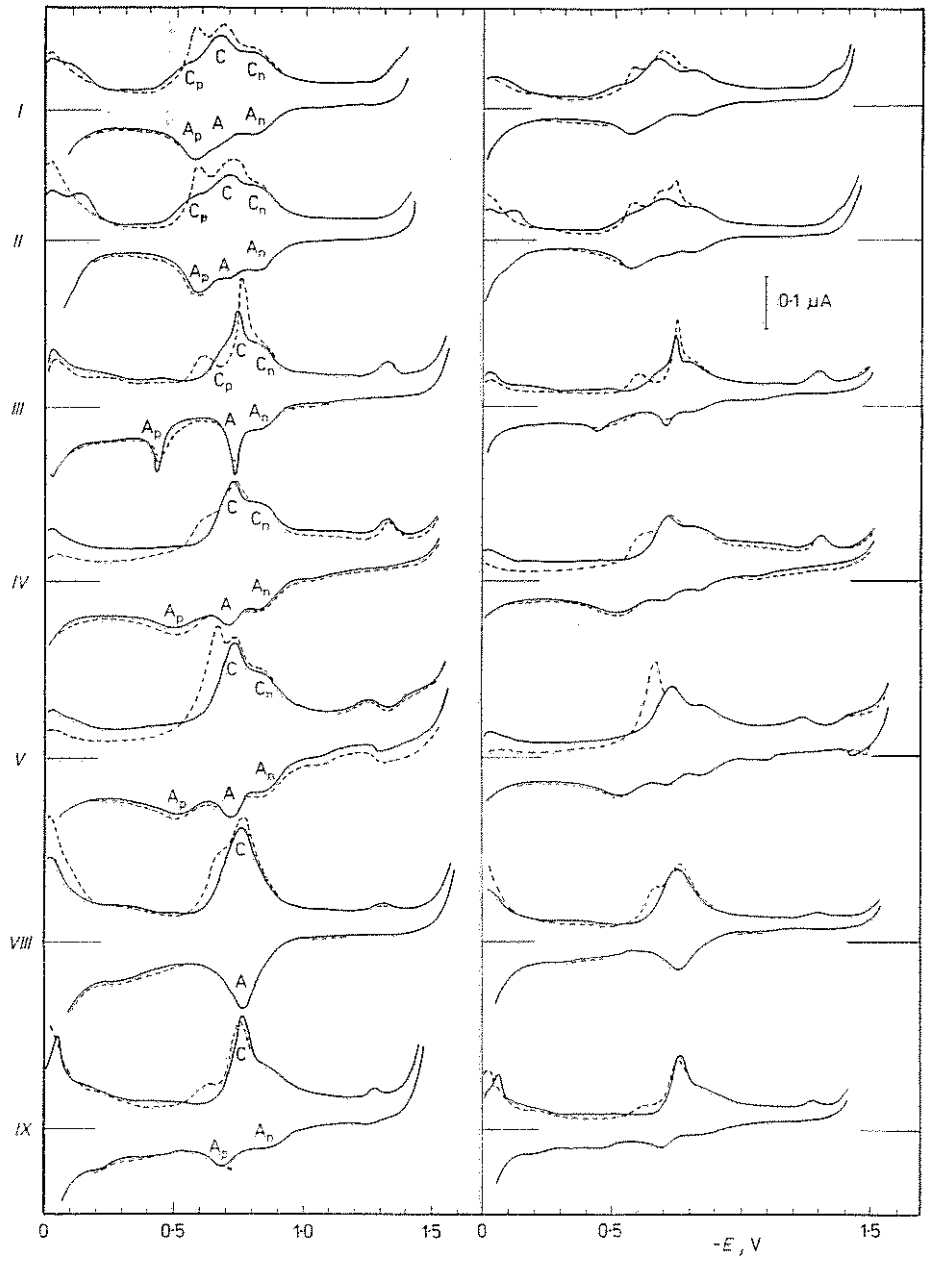

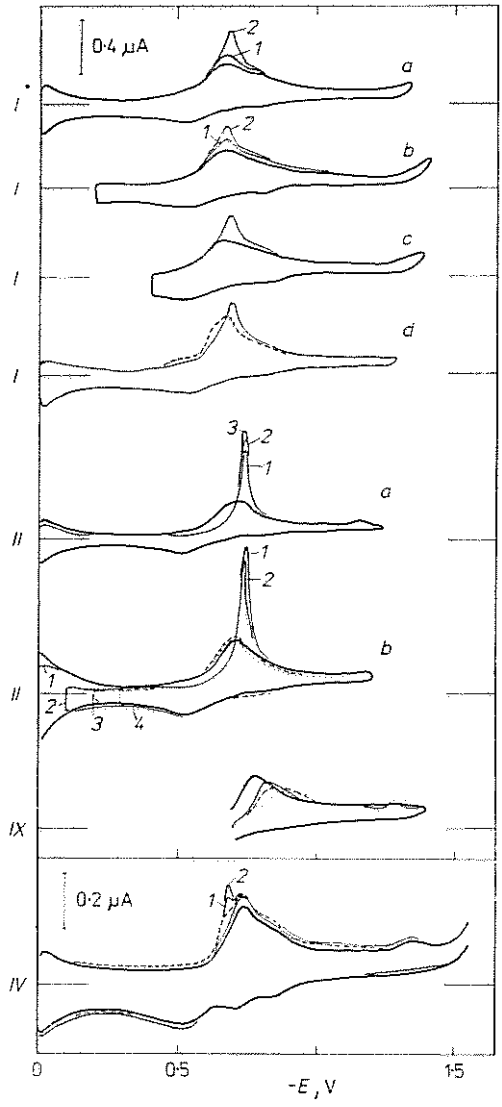

FIG. 5

Cyclic voltammograms at pH 7·4. Effect of cummulation time of the peptide at the electrode surface before starting the scan. 1st cycle. Peptide concentration (in 10^{-5} mol. l^{-1}): (*I*, *II*, *IX*) 10; (*IV*) 8. Scan rate (in mV s^{-1}): *II-a* 50; otherwise 100. With the exception of *I-d* (– – – –) and *IV* (curve 2) no stirring of the solution. *I-a*: cummulation at 0 V, cummulation time (s): (———) 0; *1* 20; *2* 120. *I-b*: cummulation at −0·2 V, cummulation time(s): (———) 0; *1* 20; *2* 80. *I-c*: cummulation at −0·4 V, cummulation time (s): (———) 0; (– – – –) 40. *I-d*: cummulation at 0 V: (———) 120 s without stirring; (– – – –) 60 s stirring + additional 60 s without stirring. *II-a*: (———) without cummulation; otherwise always cummulation for 40 s at potential (V): *1* 0; *2* −0·1; *3* −0·2; *4* −0·3. *IX*: cummulation at −0·7 V, cummulation time (s): (———) 0; (———) 20; (– – – –) 40; (...) 60. *IV*: cummulation at 0 V: (———) 0; (———) 20; (– – – –) 120; *1* 240 s; *2* 60 s stirring + additional 60 s without stirring

←

FIG. 4

Cyclic voltammograms at pH 7·4. Peptide concentration $3 \cdot 10^{-5}$ mol l^{-1}. Scan rate (in mV s^{-1}): left 100, right 50. (———) 1st cycle; (– – – –) 2nd cycle. C, A — main cathodic and anodic peak, respectively; C_n, A_n — "shoulders" at more negative potentials; C_p, A_p — "shoulders" or peaks at less negative potentials than the potentials of the main peaks C and A, respectively

In our studies with the peptides *I*, *II*, *III*, *IV*, *V*, *VIII*, and *IX*, we applied alternating voltage of the amplitude 10 mV and frequency 230 Hz; with peptides *VIa*, *VIb*,

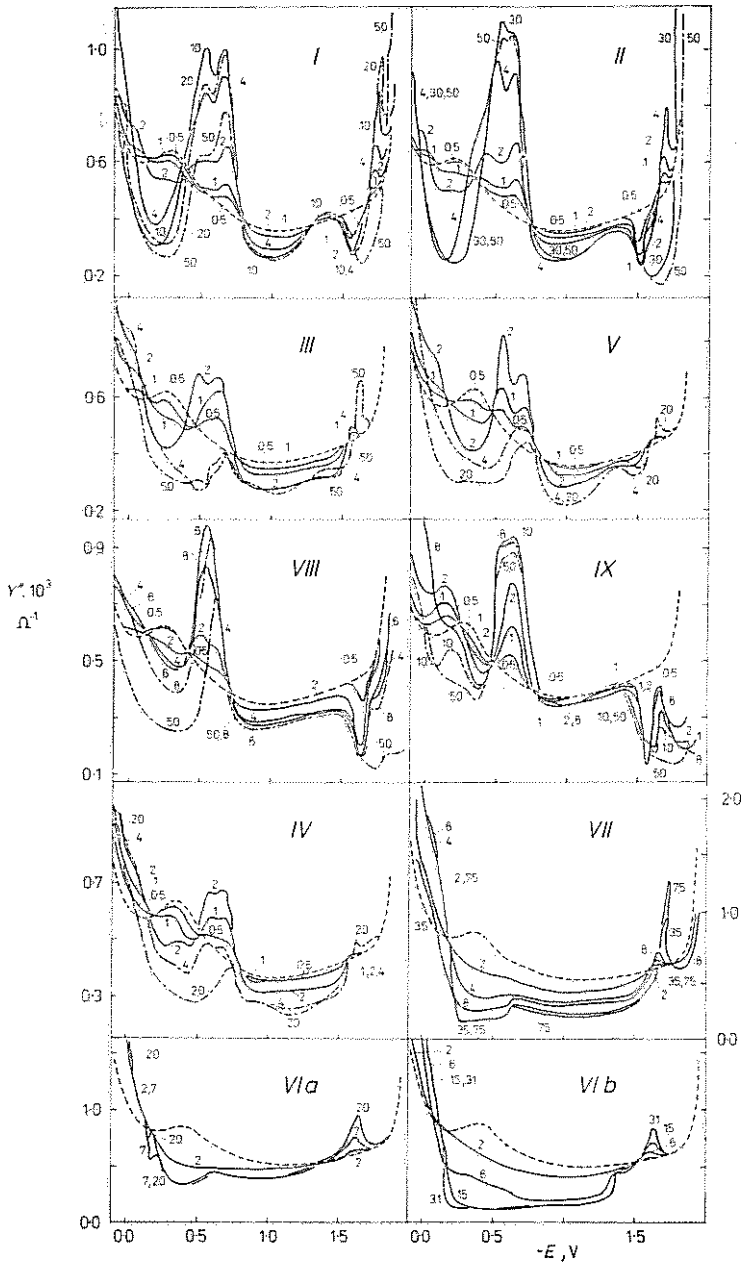

and *VII*, the above quantities were 20 mV and 290 Hz. Borate buffer of pH 7·4 served as a blank electrolyte.

Curves of the component of the electrode admittance, which was 90° phase shifted as compared to the superimposed alternating voltage (further: capacity curves) in accessible region of the applied d.c. potential (c. +0·1 to −1·8 V) exhibited in the presence of peptides characteristic changes in five different potential regions. Below, we denote these five regions as region RE (around the potential of the reference electrode), region ZC (zero-charge), region SS (reduction of the disulfide group), region MN (more negative than the SS-region), and region HH (catalyzed evolution of hydrogen). In each of these five regions, smaller or larger individual differences between the peptides were found (Fig. 6).

In the RE-region, with all peptides the admittance increases in comparison with the blank. This increase is often restricted to the lower peptide concentrations and is reversed above certain concentration of the peptide (Fig. 6, peptides *I*, *III*, *V*, *VIII*, and *IX*). The effect is most pronounced with peptide *IX* (here the increase of admittance extends even to the ZC-region) and is the smallest with peptide *II*.

In the ZC-region, we observed pronounced lowering of the electrode admittance with all peptides (relatively the least with peptide *IX*); this lowering becomes more pronounced upon increase of the peptide concentration. Sometimes (peptide *VIII*) the above change is regular, in other cases (peptides *I* and *II*) a distinct jump between the concentrations of the peptides of 2 and $4 . 10^{-5}$ mol l^{-1} has been observed.

In the SS-region (around −0·6 V) the distinct pseudocapacitance peak is present, which is obviously missing in carba-analogs (Fig. 6). For vasopressin derivatives, the peak is mostly simple and symmetrical and only occasionally it exhibits a sign of splitting. With oxytocin and its derivatives, the above peak is always distinctly split. Upon increasing the peptide concentration the peak initially grows but later decreases, the detailed course is, however, characteristically different for different peptide groups. With peptides *III*, *IV*, and *V*, the highest peak is observed at the peptide concentration $2 . 10^{-5}$ mol l^{-1} and already at $4 . 10^{-5}$ mol l^{-1} peptide it becomes considerably suppressed, almost (with peptide *III* entirely) to the level of the admittance of the blank. With the other peptides, the above inversion occurs at higher peptide concentrations (6, 8, 10 or $30 . 10^{-5}$ mol l^{-1}) and the subsequent decrease of the peak is slow. With carba-analogs the discussed potential region

←

FIG. 6

AC polarograms at pH 7·4. Dependence of the phase shifted component (90°) of the electrode admittancy (Y'') on peptide concentration. Electrode potential (E) for peptides *VIa*, *VIb*, and *VII* against SCE, otherwise against Ag/AgCl/sat. KCl. Amplitude (in mV) and frequency (in Hz) of the superimposed alternating voltage was 20 and 290 for peptides *VIa*, *VIb*, and *VII*, otherwise 10 and 230. Numbers at curves denote peptide concentration (in 10^{-5} mol l^{-1}); (-----) blank. Values of currents at the end of the drop time (4 s)

(around −0·6 V) is not influenced by the pseudocapacitance peak and the changes of admittance with peptide concentration preserve here the trend from the preceding potential region ZC, i.e., with increasing peptide concentration the admittance monotonously decreases to a limit. Each of the three carba-analogs *VIa*, *VIb*, and *VII* yields its characteristic shape of the curves (Fig. 6).

Also in the MN-region the curves monotonously fall towards the limit below the curve for the blank. The only exception is peptide *IX*, whose capacity curves differ negligibly from those of the blank.

The effect of frequency (21, 80, 230, 460, and 770 Hz) was studied with peptides *I*, *II*, *III*, *VIII*, and *IX* in concentration $2 . 10^{-5}$ mol l^{-1} in borate buffer, pH 7·4. Absolute values of the admittance in all cases rose with increasing frequency (e.g., at the potential of zero charge the values of the phase shifted component of the electrode admittance in basic electrolyte is $6 . 10^{-5}\ \Omega^{-1}$ for 21 Hz and $2 . 10^{-3}\ \Omega^{-1}$ for 770 Hz). Compared to the blank, with increasing frequency the pseudocapacitance peak corresponding to the SS-reduction becomes less distinct; similarly, smaller

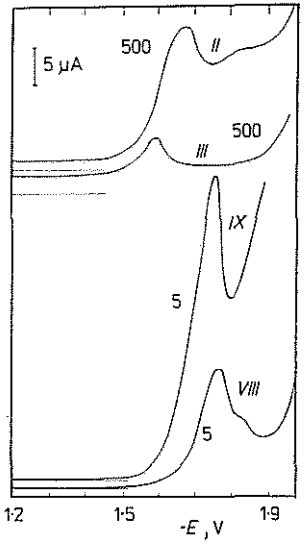

FIG. 7

DC-polarograms of the catalytic hydrogen waves. Mean currents. 0·06 mol l^{-1} borax, pH 9·2. Numbers at curves denote peptide concentration (in μmol l^{-1})

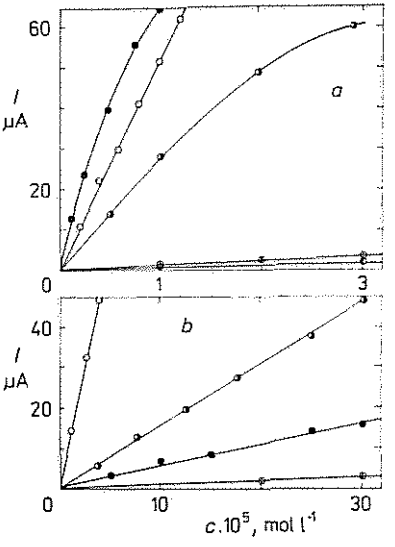

FIG. 8

Concentration dependence of the catalytic hydrogen current of peptides at different pH values. 0·12 mol l^{-1} borate buffer. *a* Peptide, pH: ● *IX*, 9·2; ⊙ *VIII*, 8·2; ◑ *VIII*, 9·2; ⊕ *VIII*, 10·2; ◐ *VIII*, 11·2. *b* Peptide, pH: ⊙ *II*, 8·2; ◑ *II*, 9·2; ● *III*, 9·2; ⊕ *II*, 10·2

differences between the capacity curves for blank alone and for blank plus peptide have been observed in the potential region RE at higher frequencies.

Catalyzed Evolution of Hydrogen

DC-*polarography*: With the exception of the carba-analogs all studied peptides yielded well pronounced catalytic hydrogen waves at potentials preceding those of the blank decomposition. By far the highest catalytic hydrogen currents are produced by the vasopressin analogs (peptides *VIII* and *IX*, see Fig. 7). From the oxytocin group, peptides *I* and *II* are most active; the activity of the other oxytocin analogs is much less, that of the carba-analogs being virtualy zero.

The catalytic hydrogen activity of the peptides *II*, *III*, *VIII*, and *IX* has been studied in more detail. With increasing peptide concentration, the catalytic hydrogen maximum (or a double maximum) is shifted somewhat to more negative potentials and its height increases, though not always linearly (Fig. 8).

With decreasing pH (between pH 11·0 and 7·3) the potentials of both catalytic maxima in borate buffers are slightly shifted to more negative values and their height increases (examples for peptides *II* and *VIII* see in Fig. 9). At pH 8·2 and less

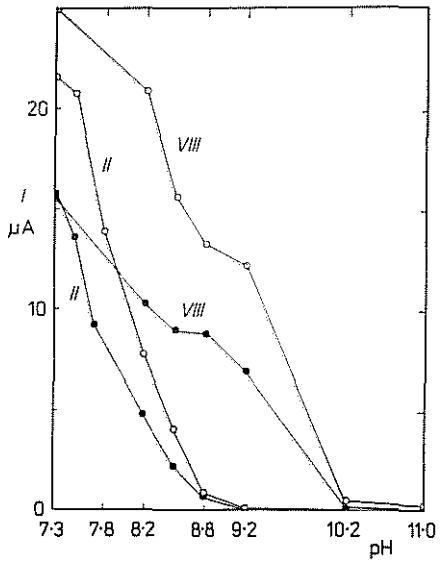

FIG. 9

Effect of pH on the catalytic hydrogen current of $1 \cdot 10^{-5}$ mol l^{-1} peptides *II* and *VIII*. ○ 1st maximum, ● 2nd maximum

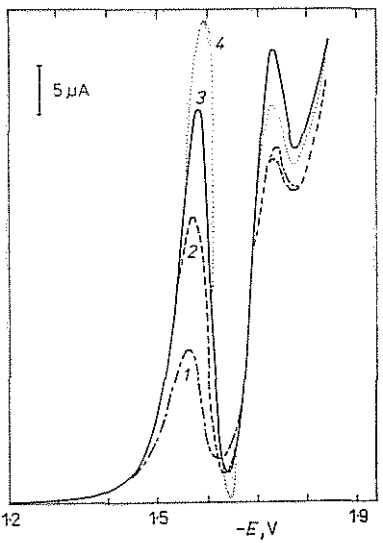

FIG. 10

DP-polarograms of the catalytic hydrogen current of peptide *II*. 0·06 mol l^{-1} borax, pH 9·2. Concentration of peptide *II* (in 10^{-5} mol l^{-1}): *1* 2·5; *2* 5; *3* 7·5; *4* 10

and at potentials −1·7 V or more negative the surface of the mercury electrode becomes soon covered by many gas bubbles.

The character of the catalytic hydrogen current of the peptides was elucidated from the studies of their dependence on temperature and on the height of the mercury reservoir; the instantaneous current vs time curves have also been recorded. With increasing height of the reservoir, the catalytic current is either practically unchanged (peptide *III*), or even decreases (peptides *VIII* and *IX*). Temperature coefficient of the catalytic hydrogen current has the value $+0{\cdot}4\%\ K^{-1}$ for peptide *III* and $+1{\cdot}2\%\ K^{-1}$ for peptide *IX*. Current–time curves were measured at various potentials of the catalytic hydrogen wave of the peptides *III* and *VIII*. Values of the exponent, x, in the expression $i = kt^x$, for peptide *VIII* were 0·80 at −1·74 V, 0·83 at −1·87 V, and 0·63 at −1·95 V.

DP-*polarography*: DP-polarograms at potentials of the catalytic hydrogen wave have been recorded with peptide *II* only (Fig. 10). While the height of the less negative DP-peak increases with increasing peptide *II* concentration, that of the more negative DP-peak varies non-monotonously. The potentials of both DP-peaks are c. 100 to 130 mV less negative than the corresponding DC-maxima.

AC-*polarography*: Capacity curves in the HH-region show characteristic differences between the groups of peptides (Fig. 6). The derivatives of vasopressin (peptides *VIII* and *IX*), and also two of the oxytocin analogs (those which have the α-NH_2 group, i.e., peptides *I* and *II*) exhibit considerable decrease of the electrode admittance in the shape of a peak (in the following, dip); this dip is obvious already

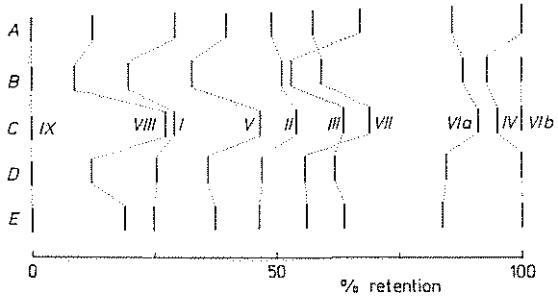

FIG. 11

Comparison of the predicted and experimentally determined elution times in chromatography on reversed phase. Retentions are given in relative scale — 0% for the most quickly and 100% for the most slowly eluted peptide. *A* Prediction according to Meek[20], 0·1 mol l^{-1} NaH_2PO_4, pH 7·4; *B* experiment, pH 7·5; *C* experiment, pH 2·2; *D* prediction according to Meek and Rossetti[21], 0·1 mol l^{-1} NaH_2PO_4 + 0·2% H_3PO_4; *E* prediction according to Browne et al.[22]

at the peptide concentration $5 . 10^{-5}$ mol l^{-1} (Fig. 6). At more negative potentials than those of the dip the peptides *I* and *II* show distinct peak which increases the admittance compared to that of the blank, but with peptides *VIII* and *IX* the latter peak is missing. Remaining peptides (oxytocine analogs with the modified or completely absent α-NH_2 group and the carba-analogs) do not show any dip; the peak which increases the admittance compared to the blank is, however, always present (Fig. 6, peptides *III*, *IV*, *V*, *VIa*, *VIb*, *VII*).

As concerns the effect of frequency, with peptide *III* the characteristic shape without the dip is frequency-independent; the dip of peptides *I*, *II*, *VIII*, and *IX* is more pronounced at higher frequencies.

Liquid Chromatography

The polarographic measurements have been compared with chromatographic separation of the ten peptides on the reversed phase at pH 2·2 and 7·5. The sequence of the peptides in both cases was identical: first eluted (i.e., the least hydrophobic) was peptide *IX*, which was followed by peptides *VIII*, *I*, *V*, *II*, *III*, *VII*, *VIa*, *IV* and the most hydrophobic peptide *VIb*. Fig. 11 shows comparison of the above behavior with that predicted by us on the basis of individual structural contributions published in refs[20-22] and completed by our own calculations of several missing data (details see below). We did not attempt to predict the behavior of peptide *VIb* because of difficulties in estimation of the influence of the D-amino acid.

DISCUSSION

There are three general causes for the changed behavior of the peptide molecules after their transfer from the bulk of the solution to the vicinity of the mercury electrode:

a) Increase in local concentration of the peptides due ot their partial pull-out from the bulk of the polar aqueous phase to any interface. Pulled-out molecules may be expected to be oriented towards the outside of the solution (i.e., towards the mercury electrode) predominantly by their hydrophobic parts, in the first place by the S—S or S-carba groups, in peptides *II*, *III*, *IV*, and *VII* also by the aromatic nucleus with methylated OH-group and, in peptides *VIII* and *IX*, also by the aromate of Phe (3rd amino acid).

b) Mercury has strong chemical affinity towards sulfur, particularly when the latter is in the form of the S—S group (see, e.g., ref.[23]). This interaction only further strengthens the already existing orientation of the S—S or S-carba group towards the surface of the mercury electrode.

c) Electrical charge of the electrode brings about changes in orientation of water dipoles nad electrostatic attraction or repulsion between the charged electrode

surface and positively charged groups in the peptide molecules (Arg^8 in peptide *VIII*, Lys^8 in peptide *IX*, terminal NH_2-group in peptide *IX*, depending on pH). These groups are polar and very flexible and, at the potential of zero charge, they can be expected to be oriented from the electrode into the solution.

Experimentally observed behavior of the studied peptides *at the potential of zero charge* corresponds very well to the above presented considerations. The hydrophobicity of the molecule plays here the decisive role. The important polar group is the OH-group in Tyr and its methylation in peptides *II*, *III*, *IV*, and *VIII* or its replacement by the C_2H_5-group in peptides *VIa* and *VIb* necessarily lead to the increase of the hydrophobicity of the whole molecule. The removal of the α-amino group in deamino analogs (peptides *V*, *VIa*, *VIb*, *VII*, *VIII*) has an analogous effect. The more hydrophobic peptides can be expected to be more strongly pulled into all interfaces, including the interface water/mercury electrode. On the basis of the presence or absence of polar (OH, NH_2) and electrically charged groups (side chain basic groups of Lys and Arg, terminal amino group of triglycyl) all the studied peptides may be arranged according to the increasing hydrophobicity as shown in Fig. 11. There exist many publications which evaluate the contributions of individual amino acid residues to the overall hydrophobicity of the peptide (for a review see ref.[24]). Our estimations are largely based on contributions determined by Meek[20], Meek and Rossetti[21], and Brown[22], since these authors have used most similar chromatographic conditions to those in our study and their sets also contain the largest number of various structural features. However, in addition we had to calculate the contributions of several not tabulated groups, i.e.: the deamination on the N-terminal amino acid; the methylation of the hydroxyl of tyrosine or its replacement by ethyl group; the carba-substitution of the disulfide bridge; the acylation of the α-amino group by the pivaloyl residue. The contribution of the deamination has been calculated from the difference of the influence of the amino-terminal glycine and the acetyl group. Influence of substitution of the tyrosine hydroxyl was calculated in accordance with ref.[25] which shows a correlation of the π-values of substituents of the tyrosine aromatic ring in the oxytocin analogs with their chromatographic behavior. The effect of carba substitution was derived experimentally from the chromatographic behavior of the set of carba-analogs[26]. The contribution of the pivaloyl group was calculated as a combination of the values of two methyl groups and an acetyl residue. The values of the obtained contributions are listed in Table III. Unfortunately, it was not possible to include the contribution of the different configuration of the amino acid residue, even though we can assume very roughly that the introduction of the D-amino acid into the molecule leads to the increased retention on reversed phase. In the study of diastereometric analogs it was found that the change of configuration in position 8 of vasopressin increased the hydrophobicity of the analog much less than the configurational change of leucine in position 8 of oxytocin or the same change in position 1 (cysteine) or 2 (tyrosine) in both

hormones (the latter behavior concerns also the peptides *VIa* and *VIb* studied in this paper). All chromatographic data suport the idea of interaction of sulfur in position 6 with the tyrosine moiety in position 2 of oxytocin. In the cases of peptides *VIa* and *VIb* the interaction of cysteine with aromate is disturbed and the aromatic moiety is freed for the interaction with lipophilic stationary phase. The agreement of predicted and experimentally obtained data at two pH values (2·2 and 7·5) shown in Fig. 11 confirms the high prediction ability of the used methods. The only change in the sequence of actual elution vs the theory (i.e., the peptides *III* and *VII*) may be explained either by overestimation of lipophilicity of the acetyl residue by the theory, or by the fact that the substitution of α-amino group by acetyl significantly changes the conformation of the analog and, as a consequence, also the energetic parameters of its interaction with the stationary phase. The largest absolute deviation from the theory is exhibited by the peptide *VIII* which, however, contains D-arginine and a change of the configuration has not been included in our calculation.

The sequence of peptides shown in Fig. 11 corresponds very well also with the order in which these peptides in low concentrations lower the electrode admittance Y'' at the zero charge potential, as compared with the value for the basic electrolyte. Thus, e.g., for peptide concentration $2 \cdot 10^{-5}$ mol l^{-1} the following values of $\Delta Y''$ ($.10^3\ \Omega^{-1}$) have been derived from Fig. 6:

$$0{\cdot}047\,(IX) < 0{\cdot}063\,(VIII) < 0{\cdot}110\,(I) < 0{\cdot}118\,(II) < 0{\cdot}157\,(IV) < \\ < 0{\cdot}204\,(III) < 0{\cdot}220\,(V) < 0{\cdot}274\,(VIb) < 0{\cdot}313\,(VIa, VII)\,.$$

TABLE III

Contribution of individual structural elements to the retention of the peptides on reversed phase (retention coefficients)

Structural element	Ref. 21		Ref. 20		Ref. 22
	min[a]	min[b]	min[c]	min[d]	% CH_3CN[e]
Deamino	6·8	3·6	2·6	5·6	11·4
Tyr(Me)	13	12·2	13·5	12·7	18·4
Phe(Et)	22·4	21·4	22·4	23·8	39·4
Pivaloyl	16·3	13·4	13·2	16·3	31·8
1-Carba[f]	−0·6	−0·6	−0·6	−0·7	−1·4
6-Carba[f]	−2·4	−2·4	−2·4	−2·8	−5·6

[a] Bio Rad ODS, linear gradient of CH_3CN (0·75% min^{-1}); buffer 0·1M-$NaClO_4$ + 0·1% H_3PO_4. [b] As in note[a] but buffer 0·1M-NaH_2PO_4 + 0·2% H_3PO_4. [c] As in note[a] but buffer 0·1M-$NaClO_4$, pH 2·1. [d] As in note[a] but buffer 0·1M-$NaClO_4$, pH 7·4. [e] Waters C_{18} μBondapak, linear gradient of CH_3CN (0·33% min^{-1}); buffer 0·1% TFA. [f] Retention should be calculated for cysteine containing compound and corrected by the given value.

Evidently, hydrophobicity has a decisive influence on the behavior of peptides in the mercury/solution interface at the potential of zero charge. The contribution due to the chemical attraction between the sulfur atoms of the disulfide group and the mercury atoms of the electrode is obviously similar for different peptides: replacement of one sulfur atom by carbon in carba analogs seems to have further positive influence on the surface excess of the peptide in the water/mercury interface. Electrostatic interactions between the peptides and the electrode do not occur at the zero charge potential. The only two anomalies between the sequences which follow from the HPLC and from the AC-polarographic behavior occurred in case of the peptides *IV* and *V*. From the chromatographic behavior it follows that the hydrophobicity of peptide *IV* is very high, even higher than that of the carba analog *VIa*, but the AC--polarography recorded only a relatively small lowering of the electrode capacity (less than with peptides *III*, *V*, *VIa*, *VIb*, and *VII*). We believe that just with this peptide *IV* the chemical attraction between sulfur and mercury cannot occur for steric reasons. On the other hand, with peptide *V* the S—S group is most exposed, what evidently leads to a stronger interaction of this peptide *V* with mercury atoms of the working electrode than, e.g., in case of peptides *II* or *III*. Both these deviations in behavior of peptides *IV* and *V* from the otherwise identical sequence of HPLC and AC-polarography support the conclusion which also stems from the DC-polarographic behavior, i.e., that the chemical interaction between the atoms of sulfur and mercury at the zero charge potential does occur and that its alteration may further support, or weaken, the contribution due to the hydrophobicity of the whole molecule of the peptide.

Transition from the potential of zero charge to the *region of the positively charged electrode* surface brings about electrostatic repulsion of the positively charged groups in peptides *VIII* and *IX*; with regard to the flexibility and polarity of these groups, it should not significantly influence orientation of the molecules of these two peptides in the interface. Their surface excess, however, may be negatively influenced, as confirmed by the results of DC-polarography. As follows from Fig. 6 for all peptides the imaginary component of the admittance of the mercury electrode increases above the curve for the basic electrolyte at potentials close to the potential of the reference electrode. Under these conditions the peptides at the interface lose the character of a passive dielectric and their specific interaction with the surface becomes the decisive factor for their behavior at the mercury electrode. The cathodic current accompanying the adsorption of the peptides at the positively charged electrode indicates that the interaction has the character of a surface bond, to which electrons are contributed by the electrode – presumably the chemical bond between sulfur and mercury is created where the electrons are shared by both partners. This interaction is not related to the electroreduction as it occurs both with the S—S and the nonreducible monosulfidic peptides. The electrode which shares electrons with the adsorbing substance cannot have an increased tendency to send free cations

into the solution – consequently the more strongly interacting peptide *VII* does not affect the dissolution of mercury and, on the other hand, the peptides which interact less strongly (e.g., peptides *VIII* and *IX*) enhance somewhat the dissolution of mercury. The formation of compounds between the peptides and mercury ions in the solutions is obviously not energetically more favoured than the surface interaction.

In potential *region of the* S—S *group reduction* we have to deal with both the original (S—S) and electroreduced (SH) forms of the peptides. AC-polarography clearly shows (Fig. 6) that both these forms are adsorbed at the electrode. On voltammetric curves, (Fig 4) the electroreduction is accompanied by two pairs of peaks: C–A and C_n–A_n. Since the electroreduction of the S—S bond occurs reversibly as a surface process under the influence of the specific interaction with mercury[23], the main peaks C and A belong to the reversible reduction of the adsorbed peptide with its sulfur atoms in contact with the electrode. With respect to their shape and symmetry, we ascribe the more negative pair of peaks C_n–A_n to the change of the capacity of the mercury electrode connected with the electrode reaction. It marks the positive limit of adsorption of the electroreduction product, since the reduction product which is formed in the interaction with mercury is itself also adsorbed. With peptide *VIII* probably the couples C–C_n and A–A_n merge into two broad peaks. In the reverse phase of the voltammetric cycle part of the reduced peptide in the adsorbed state is oxidized into the original S—S form and another part facilitates the dissolution of mercury from the electrode (peak A_p). This results in formation of a new species which is sparingly soluble and adsorbs at the electrode surface. Mercury gets reduced from this compound in the second voltammetric cycle (dashed curves in Fig. 4).

Experimental results clearly show that the course of the electroreduction of the cystine disulfidic group differs in individual peptides. This is not surprising in view of the different conformation and adsorptivity of the SS- and SH-forms at the electrode, which cause different reactivity in surface processes accompanying transfer of electrons between the electrode and the peptide. Table II gives evidence that, in principle, the conditions for the peptide reduction at the dropping and hanging mercury electrodes are not comparable. It is given by the different time periods for which the electrodes are exposed to the solution, and also by the different regimes of their polarization. At low peptide concentrations the adsorption equilibrium cannot be established during the 4 seconds of the drop life-time. Increase in peptide concentration initially accelerates establishment of this equilibrium already within the life-time of one drop; later, however, the inhibiton of adsorption on the electrode process proper becomes effective. On the hanging drop, due to the time factor the establishment of adsorption equilibrium and inhibition effects occur at lower peptide concentrations, the adsorption equilibrium being disturbed upon the change of the electrode potential. The sharp peak observed under the particular conditions on the voltammetric curves of peptides *II* and *III* shows that, as a part of adsorption of these

peptides and/or their reduction products, compact oriented layers on the electrode surface are formed.

Situation in the electrode interface within the potential *region between* c. −0·8 *and* −1·5 V, i.e., between the reduction of the S—S bond and the catalyzed hydrogen evolution (region MN), is fundamentally different for peptides containing cystine and for the nonreducible carba analogs of oxytocin. Peptides *VIa*, *VIb*, and *VII*, which do not undergo reduction, arrive by diffusion from the solution and get adsorbed on the electrode. With the other peptides the electrode is being covered by the products of the electroreduction which diffuse away from the electrode into the solution after the coverage is complete. In both cases the orientation of the substances in the adsorbed state is again determined largely by the interaction of the sulfur atoms with the surface of mercury. With regard to the strong affinity of sulfur towards mercury it is probable that the adsorption is not reversible in the whole potential range and, hence, the consideration about the adsorption equilibrium is not always justified; exact electrocapillary measurements would help to solve this question. The AC-polarographic curves in Fig. 6 do not give a strictly rigorous picture of the adsorption of the peptides and their reduction products on mercury; however, for comparison of the adsorptivities a comparison of the course of the curves for the different compounds is quite adequate.

Upon transition from the positively to the negatively charged electrode, the carba analogs obviously undergo a change in their adsorption, brought about by the change in peptide conformation in the interface. Conspicuous is the difference between the curves of the optical isomers *VIa* and *VIb* reflecting their different orientation at the electrode surface over a wide range of potentials.

As can be judged from the AC-polarographic curves of the reducible peptides, particularly striking is the weak adsorption of the reduction product of peptide *IX* in comparison with the related peptide *VIII*, the difference being obviously caused by the introduction of the bulky substituent into the neighbourhood of the S—S bond so that the contact between sulfur and mercury is sterically not convenient for interaction. The peak which exceeds the curve for basic electrolyte at negative potentials marks the final desorption of the peptide or of its reduction product from the electrode surface under the influence of the strong electric field. The absence of this peak on the curves of peptides *VIII* and *IX* is connected with the fact that, with these two peptides, a relatively strong electrolytic current due to hydrogen evolution flows through the electrode in the region of the negative potentials where the other peptides display the peak. In such case, with the apparatus used in this study, the AC-curves lose the physical meaning which they have under the pasage of no or only small Faradaic currents.

From the considerable influence of pH on the currents observed in the potential *region* HH (examples for peptides *II*, *III*, *VIII*, and *IX* see in Figs 8 and 9) it may be concluded that these currents are the catalytic currents of hydrogen. This con-

clusion is supported by the observation that at higher current densities (lower pH or higher concentration of the peptide) the surface of the mercury electrode becomes soon covered by gas bubbles.

The high catalytic hydrogen activity of the vasopressin analogs at pH 9·2 which exceeds that of peptides *II* and *III* by two orders of magnitude when measured by current (see Fig. 7) has to be ascribed to the side, nitrogen-containing groups of arginine in peptide *VIII* or lysine in peptide *IX*; their p*K* values are 12·48 (Arg) and 10·53 (Lys, see ref.[8]). In peptide *IX* the partly protonated terminal group of triglycyl (p*K* 8–9) may as well contribute to some extent to the resulting catalytic hydrogen activity.

The bearer of the above activity of peptides *I* and *II* is the α-amino group. Since its p*K* is considerably lower than that of the nitrogen-containing groups in Lys or Arg (e.g., for peptide *I* the literature gives the value 6·3) the activity of peptides *I* or *II* becomes comparable to that of peptides *VIII* or *IX* only at lower pH values (for example of peptides *II* and *VIII* see Fig. 9).

Further decrease in the catalytic hydrogen activity of peptides *III*, *IV*, and *V* is obviously connected with the substitution of the terminal α-amino group (peptides *III* and *IV*) or its complete removal (peptide *V*).

In all above-discussed peptides the SH groups formed after the reduction of the disulfide bond may as well contribute somewhat to the overall catalytic hydrogen activity of these peptides. The pK_a of these SH groups may be expected close to 8·5 (see, e.g., ref.[27]).

The catalytic hydrogen activity of the carba analogs is virtually zero even in solutions of relatively low pH values and it manifests itself only as a slight shift of the blank decomposition currents towards less negative potentials.

In the literature the possible role of sulfur in the catalytic mechanism of the polarographic reduction of hydrogen from the protein- or peptide-containing solutions has been discussed. Our results suggest that the protonizable N-groups play a dominant role. However, the practically complete absence of catalytic hydrogen activity in the carba analogs and, on the other hand, the relatively considerable activity of peptide *V* both suggest a possible participation of sulfur, either direct (hydrogen reduction from the protonated SH group) or indirect (interaction of sulfur from the SH or S^- group with the mercury electrode, having an enhancing influence upon the magnitude of the catalytic effect).

Since the DC-catalytic hydrogen wave of peptides often has the shape of a single or a double maximum it may be concluded that the protonized forms of the peptides are relatively strongly adsorbed on the electrode surface also at potentials of the catalytic hydrogen wave; the sharp decrease of the catalytic current after its maximum peak may be explained by their desorption (example see in Fig. 7).

Participation of adsorption may also explain the observed dependences of the catalytic hydrogen current on temperature and on mercury pressure, and the values

of the exponent of the instantaneous current vs time curves. The DP-polarographic behavior of peptide *II* shows the very different character of the catalytic hydrogen current in the 1st and in the 2nd maximum (Fig. 10). Comparison of the shape of the AC-polarographic curves with the corresponding DC-polarograms permits to draw approximate conclusions about the adsorptivity of the individual substances in relation to their ability to catalyze hydrogen evolution. It seems that the more strongly adsorbed substances are weaker catalysts. The sharp dips on the curves of peptides *I* and *II* and especially *VIII* and *IX* are probably connected with the mechanism of the hydrogen evolution, which is particularly strongly catalyzed by the reduced forms of these four peptides.

If the reduced, i.e., the SH-forms of the peptides are adsorbed on the electrode even at very negative potentials (in the region HH), then these SH-forms will be adsorbed, and very probably much more strongly, also in the region SS. The splitting of the 20-member ring, which is a consequence of the polarographic reduction of the SS-group, the collapse of the 3-dimensional structure of the peptides into the statistical coil, and replacement of the strongly hydrophobic SS-group by the two strongly hydrophilic SH-groups (or, at higher pH, by two electrically charged groups S^-) all necessarily lead to a considerable suppression of the hydrophobicity of the whole molecule. If, then, the relatively little hydrophobic SH-forms of the peptides are strongly surface active even at potentials of the catalytic hydrogen wave, then we must expect high surface activity of the original SS-forms of the peptides. This conclusion is in full aggreement with all our experimental findings in this study.

Our thanks are due to Dr T. Barth from the Institute of Organic Chemistry, Czechoslovak Academy of Sciences, for providing us with five of the ten peptides investigated in this study. We are also grateful to Dr K. Markušová from the Faculty of Sciences, P. J. Šafárik University in Košice, for giving us the possibility to perform part of our measurements of cyclic voltammetry in her laboratory.

REFERENCES

1. Jošt K., Lebl M., Brtník F. (Eds): *CRC Handbook of Neurohypophyseal Hormone Analogs*, Vol. I and II. CRC Press, Boca Baton 1987.
2. Krupička J., Zaoral M.: Collect. Czech. Chem. Commun. *34*, 678 (1969).
3. Rishpon J., Miller I. R.: Bioelectrochem. Bioenerg. *2*, 215 (1975).
4. Rishpon J., Miller I. R.: J. Electroanal. Chem. Interfacial Electrochem. *65*, 453 (1975).
5. Forsman U.: Anal. Chim. Acta *156*, 43 (1984).
6. Forsman U.: Anal. Chim. Acta *166*, 141 (1984).
7. Wood S. P., Tickle I. J., Treharne A. M., Pitts J. E., Mascarenhas Y., Li J. Y., Husain J., Cooper S., Blundell T. L., Hruby V. J., Wyssbrod H. R., Buku A., Fischman A. J.: Science *232*, 633 (1986).
8. Schmidt C. L. A., Kirk P. L., Appleman W. K.: J. Biol. Chem. *88*, 285 (1930).
9. Millar G. J.: Biochem. J. *53*, 385 (1953).
10. Jošt K., Rudinger J., Šorm F.: Collect. Czech. Chem. Commun. *28*, 1706 (1963).

11. Jošt K., Šorm F.: Collect. Czech. Chem. Commun. *36*, 297 (1971).
12. Krojidlo M., Barth T., Servitová L., Dobrovský K., Jošt K., Šorm F.: Collect. Czech. Chem. Commun. *40*, 2708 (1975).
13. Hope D. B., Murti V. V. S., Du Vigneaud V.: J. Biol. Chem. *237*, 1563 (1962).
14. Lebl M., Hrbas P., Škopková J., Slaninová J., Machová A., Barth T., Jošt K.: Collect. Czech. Chem. Commun. *47*, 2540 (1982).
15. Lebl M., Barth T., Servitová L., Slaninová J., Jošt K.: Collect. Czech. Chem. Commun. *50*, 132 (1985).
16. Frič I., Kodíček M., Procházka Z., Jošt K., Bláha K.: Collect. Czech. Chem. Commun. *39*, 1290 (1974).
17. Zaoral M., Kolc J., Šorm F.: Collect. Czech. Chem. Commun. *32*, 1250 (1967).
18. Procházka Z., Krejčí I., Kupková B., Slaninová J., Bojanovská V., Prusík Z., Vosekalná I. A., Maloň P., Barth T., Frič I., Bláha K., Jošt K.: Collect. Czech. Chem. Commun. *43*, 1285 (1978).
19. Volke J.: Z. Anal. Chem. *224*, 41 (1967).
20. Meek J. L.: Proc. Natl. Acad. Sci. U.S.A. *77*, 1632 (1980).
21. Meek J. L., Rossetti Z. L.: J. Chromatogr. *211*, 15 (1981).
22. Browne C. A., Bennett H. P. J., Solomon S.: Anal. Biochem. *124*, 201 (1982).
23. Danielsson R., Johansson B. L., Nygard B., Persson B.: Chem. Scr. *20*, 19 (1982).
24. Mikeš O.: *High Performance Chromatography of Biopolymers and Biooligomers*. Elsevier, Amsterdam 1988.
25. Lebl M.: J. Chromatogr. *242*, 324 (1982).
26. Lebl M. in: *Handbook of HPLC for the Separation of Amino Acids, Peptides, and Proteins* (W. S. Hancock, Ed.), Vol. II, p. 169. CRC Press, Boca Raton 1984.
27. Danehy J. P., Parameswaran K. N.: J. Chem. Eng. Data *13*, 386 (1968).

Translated by the author (P.M.).